Numerical study of multilayer adsorption on fractal surfaces

Hao Qi,[1] Jian Ma,[2] and Po-zen Wong[1]

[1]*Department of Physics, University of Massachusetts, Amherst, Massachusetts 01003*
[2]*Department of Physics, Amherst College, Amherst, Massachusetts 01002*

We report a numerical study of van der Waals adsorption and capillary condensation effects on self-similar fractal surfaces. An assembly of uncoupled spherical pores with a power-law distribution of radii is used to model fractal surfaces with adjustable dimensions. We find that the commonly used fractal Frankel-Halsey-Hill equation systematically fails to give the correct dimension due to crossover effects, consistent with the findings of recent experiments. The effects of pore coupling and curvature dependent surface tension were also studied.

The adsorption of inert molecules on self-similar fractal surfaces has been a subject of much interest and debate for more than a decade [1]. It is generally believed that the adsorption isotherm beyond the monolayer regime follows a scaling form known as the fractal Frankel-Halsey-Hill (FHH) equation

$$N = N_0 [\ln(P_0/P)]^{-\zeta}, \qquad (1)$$

where N is the number of molecules adsorbed, P is the vapor pressure above the fractal surface, and P_0 is the saturation vapor pressure at the temperature of interest. The prefactor N_0 depends on system specific parameters such as the linear size of the surface L, the density of the film ρ, etc. The central issue has to do with how the exponent ζ depends on the fractal dimension D of the surface. Some authors have suggested that [2]

$$\zeta = (3-D)/3, \qquad (2)$$

while others have argued that [3]

$$\zeta = 3 - D. \qquad (3)$$

The difference has to do with what one believes to be the correct length scale l for measuring the volume of the adsorbed film. If the van der Waals adsorption potential is dominant, the average film thickness t on a planar surface is expected to be given by

$$\alpha a^3/t^3 = k_B T \ln(P_0/P), \qquad (4)$$

where a^3 represents the volume occupied by a liquid molecule and α is an interaction energy. If the surface tension γ between the film and the vapor is dominant, the well known Kelvin equation sets a minimum radius of curvature r for the liquid-vapor interface, given by [4,5]

$$2\gamma a^3/r = k_B T \ln(P_0/P). \qquad (5)$$

In both cases, $k_B T \ln(P_0/P)$ represents the chemical potential difference $(\mu_0 - \mu)$ between the bulk liquid and vapor phases at temperature T. Since the volume of the wetting film on self-similar surfaces is expected to scale as l^{3-D} [6], using either t or r as the length scale l leads to the two different predictions for ζ above. However, Kardar and Indekeu

pointed out that self-affine surface roughness would yet lead to a different prediction and a correct theory should include both the substrate potential and the surface tension [7]. To address this issue, we recently reported a study of nitrogen adsorption in shale with fractal pore surfaces [8]. D for each sample was independently determined by small-angle neutron scattering (SANS) [9]. We found that using Eqs. (1)–(3) to analyze the adsorption data consistently gave lower values for D and there were also noticeable systematic errors in the fits. In this paper, we report a computer simulation that is aimed at clarifying the applicability of the theory to real experiments.

Before describing our numerical study, it is necessary to review the status of the experiments briefly. We note that Eqs. (1)–(3) have been widely used to analyze adsorption isotherm data for a long time without a great deal of success. In many cases, Eq. (1) fitted the data over less than one decade of length scales [2,10]. In some cases, using Eq. (2) to interpret the exponent gave surface fractal dimension $D < 2$, which is unphysical [11]. While there have been attempts to compare different methods of analyzing the isotherm data [12], verification of the results using other techniques such as small-angle scattering were rare [13,14]. Thus the applicability of Eq. (1) to real systems has remained unclear. In Fig. 1, we replot the data from our earlier paper (Paper I) [8] to illustrate the problem. The adsorbed amount is expressed in terms of the ratio of the film volume V_{ad} to the total pore volume V_{full}. The length scale is expressed in terms of the Kelvin radius r measured in units of a (0.4 nm for N_2 molecules) and it is calculated using Eq. (5) for a range of pressure P relative to the saturation value P_0 for liquid nitrogen at 65 K, the temperature of the experiment. The fit was made over a two-decade range (0.4–50 nm) that coincides with the SANS data. Figure 1(a) shows that using a linear fit on log-log scales and interpreting the slope ($=0.46$) according to Eq. (3) give $D=2.54$, a result that is significantly less than the value 2.83 obtained by SANS. Using Eq. (2) for the slope would give an unphysical value of 1.62. The horizontal dotted line at $V_{ad}/V_{full} \approx 0.1$ represents the monolayer capacity as determined by the standard Brunauer-Emmett-Teller analysis [5] and the vertical dotted line at $r/a \approx 3$ represents the onset of hystereses between adsorption and desorption (not shown). The latter is a signature of capillary condensation in small pores due to surface
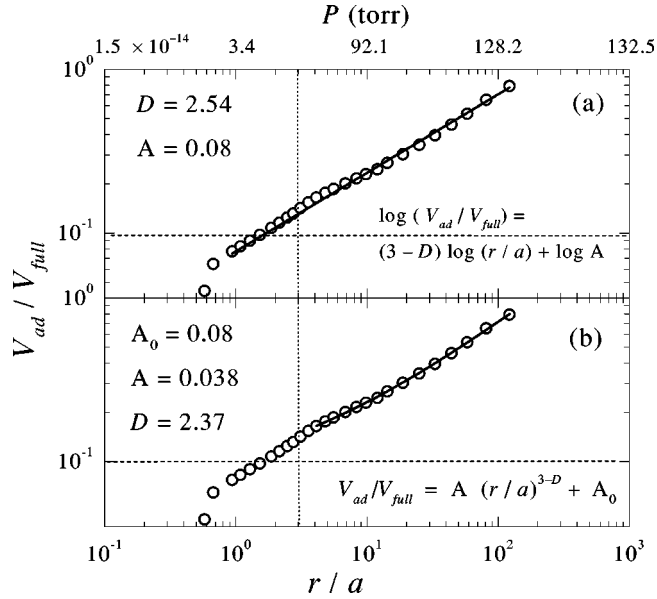
FIG. 1. Nitrogen adsorption isotherm of a shale sample with fractal pore surface. The fractal dimension D obtained by SANS is 2.83 but analyses using Eqs. (1) and (3) give much lower values. (a) A linear fit on a log-log scale over two decades of length scales gives $D = 2.54$. (b) A power-law fit of the data in the capillary condensation regime gives $D = 2.37$.
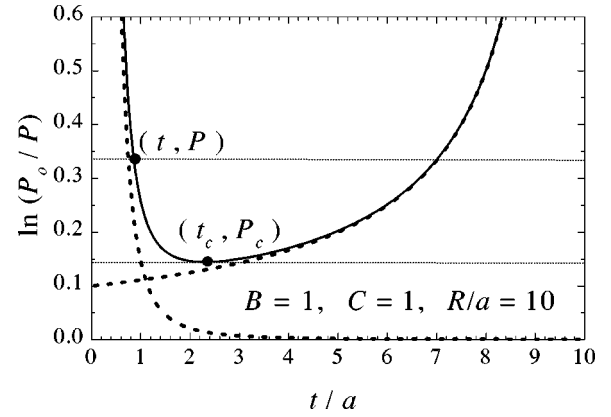

FIG. 2. A graphical representation of the solution of Eq. (6). The two dashed lines represent the two terms on the right-hand side of the equation and the solid curve is their sum. The minimum at (t_c, P_c) corresponds to the threshold of capillary condensation in a pore of radius R for the given parameters B and C. See text for details.

tension [15]. There is clearly a shoulder above the fitted line, near this point where the adsorbed volume is still less than two monolayers. At higher pressure, or longer length scales where capillary condensation is expected to be more dominant, the data show a slight upward curvature. Figure 1(b) shows that fitting only the data above the shoulder to Eq. (1) with an additive background gives $D = 2.37$, if Eq. (3) is used, which makes the disagreement with SANS worse. The same systematic deviations were seen in all three samples with different fractal dimensions [8]. We suggested in paper I that the most likely explanation was that Eqs. (1)–(3) represent asymptotic behavior that might not be observable in real systems. The crossover between van der Waals adsorption and capillary condensation would prevent such a simple analysis. The purpose of the present work is to test this hypothesis by carrying out a computer simulation using a simple model with a known fractal dimension.

The model we used to represent a fractal surface is an assembly of independent spherical pores with a power-law distribution in the radii R. If the number density follows $g(R) \propto R^{-(D+1)}$, then the surface area measured on a length scale l is $S_l \propto \int_l R^2 g(R) dR \propto l^{2-D}$, as expected of a fractal surface. Hence D can be easily adjusted without any complication in the calculation. For each pore radius R, how the film thickness t grows with increasing pressure P up to the point of capillary condensation can be calculated numerically by combining Eqs. (4) and (5) to account for both the substrate potential and the surface tension. The resulting equation in dimensionless form is

$$\ln(P_0/P) = \frac{\mu_0 - \mu}{k_B T} = B\left[\frac{a^3 R^3}{t^3(2R-t)^3} + \frac{Ca}{R-t}\right], \qquad (6)$$

where $B = 8\alpha/k_B T$ and $C = \gamma a^2/4\alpha$. The first term on the right comes from the van der Waals potential inside a spherical pore of radius R at a normal distance t from the surface and B is a measure of the adsorption energy relative to the thermal energy. The second term is due to the surface tension of a meniscus of radius $R-t$ and C is a measure of the relative strength of surface tension to the substrate potential. In real systems, B and C should be of order unity or greater when adsorption and capillary condensation occur.

The solution of Eq. (6) can be best understood using the graphical approach of Cohen et al. [16]. Figure 2 is a plot of the equation with $B = C = 1$ and $R/a = 10$. The solid line shows how the right-hand side of Eq. (6) varies with the film thickness t/a. The contributions from the two separate terms are indicated by the dashed lines. We note that while the van der Waals term falls off with increasing t, the surface tension term rises with t. Hence their sum has a minimum at the point (t_c, P_c). For any nonzero pressure P, a horizontal (dotted) line can be drawn through the point $\ln(P_0/P)$ on the vertical axis. For low pressures, the line intersects the solid curve at two points that are the solutions of Eq. (6), but the physical film thickness is given only by the smaller of the two t values. With increasing pressure, the horizontal line is shifted downward and t increases. At the critical pressure P_c, the line is tangent to the solid curve and it gives the maximum film thickness t_c, which is the threshold of condensation. At pressure above P_c, Eq. (6) has no real roots for t, i.e., the pore is filled. We can see from Fig. 2 and Eq. (6) that increasing B would shift both of the dashed lines upward, thereby lowering P_c without affecting t_c. Increasing C would shift only the dashed line on the right, thereby lowering both P_c and t_c. In our study, we varied both B and C over the range 0.1–10. Each choice of (B, C) gives a different isotherm. We chose three different D values (2.5, 2.7, and 2.85) to roughly match our earlier experiment [8].

To simulate an adsorption isotherm, we discretized the distribution function $g(R)$ with 200 values of R spaced uniformly on a logarithmic scale over three decades: $2 \leq R/a$
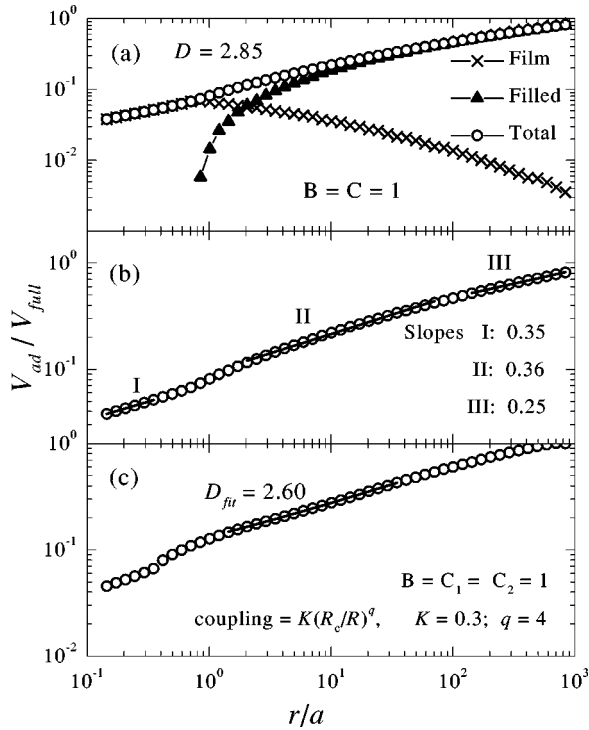
FIG. 3. Simulated isotherms for a sample with $D=2.85$ and $B=C=1$. (a) The onset of capillary condensation causes the appearance of a shoulder near $r/a\approx 1$. (b) The variation in the local slope of the isotherm is due to the crossover from the van der Waals effects (Region I) to surface tension effects (Region III). The slope in the two limits should be given by Eqs. (2) and (3), respectively. Most experiments fall in between (Region II). The correct fractal dimension is not observed in any of the three regions in this example. (c) By letting the constant C be R dependent and pores with radius $R>R_c$ to condense with a probability $K(R_c/R)^q$, the shoulder in the isotherm is accentuated.

≤ 2000. For each R, Eq. (6) can be solved to find the condensation pressure P_c. In practice, we found for each pressure P the critical radius R_c. All the pores with $R<R_c$ are filled, and for those with $R>R_c$, the film thickness t was calculated. The total adsorbed amount was obtained by summing the contributions over the power-law distribution $g(R)$. Fifty pressure steps were used to obtain the entire isotherm and the pressure range was chosen such that the Kelvin radius r in Eq. (5) spanned four decades ($0.1a$ to $1000a$), much wider than any real experiment. In Fig. 3(a), the open circles depict the simulated isotherm with $B=C=1$ for a sample with $D=2.85$, a value that matches closely to the real sample in Fig. 1. The simulation data exhibit a shoulder just above $r/a\approx 1$ in a manner similar to the real data in Fig. 1, but here we can see explicitly that it was caused by the onset of capillary condensation in the smallest pore: above this threshold, the increase of pressure (or r) causes a rapid rise in the condensed volume (solid triangles) and a corresponding decrease of the film volume (crosses). That the adsorption is separated into these two components explains why using either Eq. (2) or Eq. (3) alone to interpret the data over the entire range would result in systematic errors. At best, one should expect Eq. (2) to apply below the

condensation threshold and Eq. (3) above it.

Figure 3(b) shows how the local slope of the simulated isotherm varies in a log-log plot. In the limit of small r (Region I) where there is no condensation, the slope of $0.35\approx 1/3$ corresponds to $D\approx 2$ according to Eq. (2). This proved to be a robust result for all the cases we examined. It implies that the film thickness t given by Eq. (4) is not a length scale that could be used to probe fractal features, because t can be used only when the system is free of capillary condensation, but that guarantees it to be below the lower cutoff of the fractal features (the smallest pore size) in our model. As a result, the only possibility is to use the Kelvin radius r and analyze the data in the limit of large r, because the volume of the adsorbed film is a smaller percentage of the pore volume in the larger pores. In our simulation, we found that this approach works only for cases with large values of C and only near the upper limit of the range of r we used. In other cases, we still found fractal dimensions clearly below the true value. For example, the data in Fig. 3(b) fit a slope of 0.25 in the large r limit (Region III). It corresponds to $D=2.75$ according to Eq. (3), which is appreciably less than the input value of 2.85 used for the simulation. In the middle region (Region II) where r is comparable to the real data in Fig. 1, the slope is higher (0.36) and it results in an even lower observed dimension ($D=2.64$). This trend of disagreement is consistent with what we found between our SANS and adsorption experiments [8]. Similar behavior was observed in our simulated samples with $D=2.7$ and $D=2.5$. There is always an anomaly at the onset of capillary condensation, albeit the appearance varies somewhat. The reason is that the slope in Region I is always close to 1/3 while that in Region III varies with D. So how the data join together in the middle is not universal. For the $D=2.5$ case, the slope in Region III tends to 0.5, which is much higher than that in Region I. Hence the shoulder structure is masked by the intrinsic increase of the slope from 1/3 to 1/2, making the anomaly appear more like a kink. For $D=2.7$, although the slope in Region III tends to 0.3, a value nearly identical to that in Region I, the shoulder appearance remains pronounced.

Our model was extended in a phenomenological way to include some effects that occur in real systems. For example, the density of a liquid film is typically higher near the substrate and liquid/vapor surface tension is expected to be stronger for concave surfaces with small radius of curvature. Both of these effects would increase the second term in Eq. (6) relative to the first term. We investigated these effects qualitatively by letting C be a function $C(R)=C_1+C_2\exp(-R/\lambda)$. From the data shown in Ref. [5], we estimated that $\lambda\approx 5.4a$. In addition, for any real fractal surface, features of different sizes are not completely independent. Condensation in small pores can trigger the same to occur in neighboring large pores. We modeled such pore coupling effects by letting pores with radius $R>R_c$ to condense with a probability $K(R_c/R)^q$, i.e., less likely for larger pores. Figure 3(c) shows that with $C_1=C_2=1$, $K=0.3$, and $q=4$, the isotherm in Fig. 3(b) acquires a more pronounced shoulder. The curvature in Region II also changes from concave downward to concave upward. A power-law fit gives a slightly

lower dimension ($D = 2.60$). These results are in qualitative agreement with the real data in Fig. 1. They can be explained by the fact that the increased surface tension makes condensation in small pores to occur at a lower pressure and pore coupling makes some of the larger pores to follow. The net result is to enhance the anomaly at the onset of capillary condensation.

Despite the fact that our model is far from being realistic, it clarifies a long-standing ambiguity associated with the interpretation of adsorption isotherm on fractal surfaces. By varying the parameters B, C, and D, we are able to clearly identify the crossover between substrate driven adsorption and surface tension driven condensation. This crossover prevents one from using the FHH equation to obtain the correct fractal dimension under common experimental conditions. However, we should emphasize that the clean separation of the two mechanisms is a direct consequence of our choice of using uncoupled spherical pores in the model. For other pore shapes [15], any kind of sharp corners and creases of the surface would prevent one from describing adsorption and condensation by two distinct length scales t and r. If the pores were modeled as a connected spatial network, one would be unable to describe the phenomena in terms of the behavior in single pores. The *unrealistic* nature of the model is actually an advantage and not a shortcoming, for it enables us to understand the phenomena in simple conceptual terms. Despite the simplifications, that the resulting isotherms resemble the real data lends confidence to this understanding. Since fractal interpretations of experimental data have continued to be controversial in recent years [17] and the FHH equation has continued to be used to extract fractal dimension [10,11], we hope that the results presented here will serve as a useful reference point to add some clarity to the situation.

---

[1] See, e.g., Y. C. Yortsos, in *Methods in the Physics of Porous Media*, edited by P.-z. Wong (Academic Press, San Diego, 1999), pp. 69-117; A.V. Neimark, Russ. J. Phys. Chem. **64**, 1397 (1990); P. Pfeifer and M.W. Cole, New J. Chem. **14**, 221 (1990).

[2] P. Pfeifer, Y.J. Wu, M.W. Cole, and J. Krim, Phys. Rev. Lett. **62**, 1997 (1989).

[3] Y. Yin, Langmuir **7**, 216 (1991); B. Sahouli, S. Blacher, and F. Brouers, *ibid.* **12**, 2872 (1996); M. Jaroniec, *ibid.* **11**, 2317 (1995); D. Avnir and M. Jaroniec, *ibid.* **5**, 1431 (1989).

[4] A. W. Adamson and A. P. Gast, *Physical Chemistry of Surfaces*, 6th ed. (Wiley, New York, 1997).

[5] S. J. Gregg and K. S. W. Sing, *Adsorption, Surface Area and Porosity* (Academic, New York, 1982).

[6] See, e.g., P. G. de Gennes, in *Physics and Chemistry of Disordered Materials*, edited by D. Alder, H. Fritsche, and S. R. Ovshinsky (Plenum, New York, 1985), pp. 227-241.

[7] M. Kardar and J.O. Indekeu, Phys. Rev. Lett. **65**, 662 (1990); Europhys. Lett. **12**, 161 (1990).

[8] J. Ma, H. Qi, and P.-z. Wong, Phys. Rev. E **59**, 2049 (1999).

[9] P.-z. Wong, J. Howard, and J.S. Lin, Phys. Rev. Lett. **57**, 637 (1986).

[10] S. Blacher, R. Pirard, J.P. Pirard, B. Sahouli, and F. Brouers, Langmuir **13**, 1145 (1997).

[11] See, e.g., I.M.K. Ismail and P. Pfeifer, Langmuir **10**, 1532 (1994); B. Sahouli, S. Blacher, and F. Brouers, *ibid.* **13**, 4391 (1997).

[12] See, e.g., H. Darmstadt, C. Roy, S. Kallaguine, B. Sahouli, S. Blacher, R. Pirard, and F. Brouers, Rubber Chem. Technol. **68**, 330 (1995).

[13] See, e.g., S. K. Sinha, in *Methods in the Physics of Porous Media*, edited by P.-z. Wong (Academic Press, San Diego, 1999), pp. 223-262.

[14] B. Sahouli, S. Blacher, F. Brouers, R. Sobry, G. Van Den Bossche, B. Diez, H. Darmstadt, C. Roy, and S. Kallaguine, Carbon **34**, 633 (1996).

[15] R.M. Barrer, N. McKenzie, and J.S.S. Reay, J. Colloid Sci. **11**, 479 (1956).

[16] S.M. Cohen, R.A. Guyer, and J. Machta, Phys. Rev. B **33**, 4664 (1986).

[17] See, e.g., B.B. Mandelbrot, Science **279**, 783 (1998); P. Pfeifer, *ibid.*, **279**, 785 (1998); O. Biham, O. Malcai, D.A. Lidar, and D. Avnir, *ibid.* **279**, 785 (1998).